Online Importance Sampling for Stochastic Gradient Optimization

Corentin Salaün[1][a] Xingchang Huang[1][b] Iliyan Georgiev[2][c] Niloy Mitra[2,3][d] Gurprit Singh[1][e]

[1]*Max Planck Institute for Informatics, Saarland University, Saarbrücken, Germany*

[2]*Adobe Research, London, United Kingdom*

[3]*Department of Computer Science, University College London, London, United Kingdom*

{*csalaun,xhuang,gsingh*}*@mpi-inf.mpg.de, igeorgiev@adobe.com, n.mitra@cs.ucl.ac.uk*

arXiv:2311.14468v3 [cs.LG] 28 Jan 2025

Keywords: Optimization, Machine Learning, Gradient Estimation

Abstract: Machine learning optimization often depends on stochastic gradient descent, where the precision of gradient estimation is vital for model performance. Gradients are calculated from mini-batches formed by uniformly selecting data samples from the training dataset. However, not all data samples contribute equally to gradient estimation. To address this, various importance sampling strategies have been developed to prioritize more significant samples. Despite these advancements, all current importance sampling methods encounter challenges related to computational efficiency and seamless integration into practical machine learning pipelines. In this work, we propose a practical algorithm that efficiently computes data importance on-the-fly during training, eliminating the need for dataset preprocessing. We also introduce a novel metric based on the derivative of the loss w.r.t. the network output, designed for mini-batch importance sampling. Our metric prioritizes influential data points, thereby enhancing gradient estimation accuracy. We demonstrate the effectiveness of our approach across various applications. We first perform classification and regression tasks to demonstrate improvements in accuracy. Then, we show how our approach can also be used for *online* data pruning by identifying and discarding data samples that contribute minimally towards the training loss. This significantly reduce training time with negligible loss in the accuracy of the model.

1 Introduction

Stochastic gradient descent (SGD) combined with back-propagation has driven significant advances in optimization tasks. Its strength lies in its ability to optimize complex models by iteratively updating their parameters based on the gradient of the loss function. However, despite its widespread use, SGD has notable limitations. Convergence rates are influenced by several factors, with gradient noise being a key challenge that affects both robustness and convergence speed. Reducing this noise has been a focus of recent research (Alain et al., 2015; Faghri et al., 2020; Johnson and Zhang, 2013; Gower et al., 2020; Needell et al., 2014).

Various strategies have been proposed to mitigate gradient noise, including data diversification (Zhang et al., 2017, 2019), adaptive batch sizes, weighted sampling (Santiago et al., 2021), and importance sampling (Katharopoulos and Fleuret, 2018). These approaches aim to enhance gradient estimation and accelerate convergence in noisy optimization landscapes.

This work focuses on both importance sampling and data pruning as complementary techniques to improve training efficiency. Importance sampling involves constructing mini-batches through non-uniform data-point selection, i.e., picking certain data points with higher probability based on their expected contribution to the model's learning process. In parallel, data pruning seeks to identify and eliminate data points that contribute minimally to training, reducing computational load. This is especially beneficial in large-scale learning tasks, where reducing data complexity can significantly improve both time and resource efficiency. By jointly leveraging these two techniques, we aim to both improve the accuracy of gradient estimates and streamline the training process by focusing computation resources on valuable data.

In this paper, we introduce a novel metric that

[a] https://orcid.org/0000-0002-5112-7488
[b] https://orcid.org/0000-0002-2769-8408
[c] https://orcid.org/0000-0002-9655-2138
[d] https://orcid.org/0000-0002-2597-0914
[e] https://orcid.org/0000-0003-0970-5835

quantifies the contribution of each data sample to the model's learning process, to guide both importance sampling and data pruning decisions. Our approach leverages information from the network's output to strategically allocate computational resources to the most impactful data points. This results in substantial improvements in convergence across a variety of tasks, while sustaining minimal computational overhead compared to state-of-the-art methods that share similar goals (Katharopoulos and Fleuret, 2018; Santiago et al., 2021).

In summary, our contributions can be distilled into the following key points:

- We propose an adaptive metric for importance sampling improving gradient accuracy.
- We introduce an efficient online sampling algorithm that incorporates our metric.
- We demonstrate the effectiveness of our approach through evaluations on classification and regression problems.
- We further demonstrate the ability of our algorithm to perform online data pruning. Our approach allows using any importance function for data pruning and does not require any preprocessing of the data.

2 Related work

Gradient estimation is a cornerstone in machine learning, underpinning the optimization of models. In practical scenarios, computing the exact gradient is infeasible due to the sheer volume of data, leading to the reliance on mini-batch approximations. Improving these approximations to obtain faster and more accurate estimates remains a challenge. The ultimate goal is to accelerate gradient descent by using more accurate gradient estimates.

Importance sampling. Importance sampling serves as a mechanism for error reduction in mini-batch gradient estimation. Each data point is assigned a probability to be selected in each mini-batch, making some data more likely to be chosen than others. Bordes et al. (2005) developed an online algorithm (LASVM) which uses importance sampling to train kernelized support vector machines. Several studies have shown that importance sampling proportional to the gradient norm is the optimal sampling strategy (Zhao and Zhang, 2015; Needell et al., 2014; Wang et al., 2017; Alain et al., 2015). Hanchi et al. (2022) recently proposed deriving an importance sampling metric from the gradient norm of each data point, demonstrating favorable convergence properties and provable improvements under certain convexity conditions.

Estimating the gradient for each data point can be computationally intensive. Thus, the search for more efficient sampling strategies has led to the exploration of efficient approximations of the gradient norm. Methods proposed by Loshchilov and Hutter (2015) rank data based on their loss and derive an importance sampling strategy assigning higher importance to data with higher loss. Katharopoulos and Fleuret (2017) proposed importance sampling the loss function. Additionally, Dong et al. (2021) proposed a resampling-based algorithm to reduce the number of backpropagation computations, selecting a subset of data based on the loss. Similarly, Zhang et al. (2023) proposed resampling based on multiple heuristics to reduce the number of backward propagations and focus on more influential data. Katharopoulos and Fleuret (2018) introduced an upper bound to the gradient norm that can be used as an importance function, suggesting re-sampling data based on importance computed at the last layer. These resampling methods reduce unnecessary backward propagations but still require forward computation for each data point.

Data weighting. An alternative to importance sampling is to adjust the contribution of uniformly selected data points by a weighting factor. To compute weights within a mini-batch, Santiago et al. (2021) proposed a method maximizing the mini-batch's effective gradient. This allocation of weights aims to align data contributions with the optimization objective, expediting convergence at the cost of potential bias.

Data pruning. Data pruning reduces the computational load of training by removing minimally useful data. Early work by Har-Peled and Kushal (2005) proposed using a smaller, representative dataset for k-means clustering. This concept has expanded to other machine learning tasks, where not all data points contribute equally to learning. Toneva et al. (2019) found that some data points, once correctly classified, remain so, suggesting they can be pruned without affecting performance.

Coleman et al. (2020) introduced a proxy network to guide pruning by selecting relevant data points based on predictions. Paul et al. (2021) further refined this strategy by using early training information to identify important data points, allowing training on smaller data subsets with small performance loss. These methods show that focusing on the most infor-

mative samples can enhance training efficiency. Yang et al. (2023) proposed to select a subset of the dataset and propose a discrete optimization method using influence functions to determine which data points to retain and which to prune from the training dataset. Unfortunately, their overall preprocessing can take hours and does not scale well to large datasets. In contrast, our importance sampling algorithm can be used for *online* data pruning without any preprocessing. Qin et al. (2023) proposed an online data pruning method based on loss of data samples with an additional re-scaling of the sample gradient.

3 Background

In machine learning, the goal is to find the optimal set of parameters θ for a model function $m(x,\theta)$, with x a data sample (and y its supervision label), that minimize a loss function $\mathcal{L}$ over a dataset Ω. The optimization is typically expressed as

$$\theta^* = \underset{\theta}{\operatorname{argmin}} L_\theta, \text{ where} \tag{1}$$
$$L_\theta = \frac{1}{|\Omega|}\int_\Omega \mathcal{L}(m(x,\theta),y)\mathrm{d}(x,y) = \mathrm{E}\left[\frac{\mathcal{L}(m(x,\theta),y)}{p(x,y)}\right].$$

The total loss L_θ can be interpreted in two ways. The analytical interpretation views it as the integral of the loss $\mathcal{L}$ over a data space Ω, normalized by the space's volume. In machine learning, the data space typically represents the (discrete) training dataset and the normalization is its size. The second, statistical interpretation defines L_θ as the expected value of the loss $\mathcal{L}$ for a randomly selected data point, divided by the probability of selecting it. The two approaches are equivalent.

In practice, the minimization of the total loss L_θ is tackled via iterative gradient descent. At each iteration t, its gradient ∇L_{θ_t} with respect to the current model parameters θ_t is computed, and those parameters are updated as

$$\theta_{t+1} = \theta_t - \lambda \nabla L_{\theta_t}, \tag{2}$$

where $\lambda > 0$ is the learning rate. The learning rate does not need to remain constant throughout the iterations and can be adjusted accordingly. The procedure is repeated until a convergence criterion is met or for a predefined number of iterations.

3.1 Monte Carlo gradient estimator

Gradient estimator. The parameter update in Eq. (2) involves evaluating the total-loss gradient ∇L_{θ_t}. This requires processing the entire dataset Ω at each of potentially many (thousands of) steps, making the optimization computationally infeasible. In practice one has to resort to mini-batch gradient descent at each iteration which estimates the gradient from a small set $\{x_i\}_{i=1}^B \subset \Omega$ of randomly chosen data points from the entire dataset in a Monte Carlo fashion:

$$\nabla L_\theta \approx \frac{1}{B}\sum_{i=1}^{B}\frac{\nabla\mathcal{L}(m(x_i,\theta),y_i)}{p(x_i,y_i)} = \langle \nabla L_\theta \rangle, \text{ with } x_i \propto p(x_i). \tag{3}$$

Here, $\nabla\mathcal{L}(m(x_i,\theta),y_i)$ is the gradient (w.r.t. θ) of the loss function for sample x_i selected following a probability density function (pdf) p (or probability mass function in case of a discrete dataset). Any distribution p ensuring that $p(x) = 0 \Rightarrow \nabla\mathcal{L}(m(x_i,\theta),y_i) = 0$ yields an unbiased gradient estimator, i.e., $\mathrm{E}[\langle \nabla L_\theta \rangle] = \nabla L_\theta$. The sampling of the multiple data of a mini-batch is done with replacement to ensure all data are selected flowing the same probability density $p(x)$. Mini-batch gradient descent uses $\langle \nabla L_\theta \rangle$ in place of the true gradient ∇L_θ in Eq. (2) to update the model parameters at every optimization iteration. The batch size B is typically much smaller than the dataset, enabling practical optimization.

Theoretical convergence analysis. Mini-batch gradient descent is affected by Monte Carlo noise due to the stochastic gradient estimation in Eq. (3). This noise arises from the varying contributions of different samples x_i to the estimate and can cause the parameter optimization trajectory to be erratic, slowing down convergence. In certain conditions, it is possible to express the convergence rate of such methods. Gower et al. (2019) demonstrated that for an L-smooth and μ-convex function, the convergence rate of mini-batch gradient descent with constant learning rate is

$$\mathrm{E}\left[\|\theta_t - \theta^*\|^2\right] \leq (1-\lambda\mu)^t \|\theta_0 - \theta^*\|^2 + \frac{2\lambda\sigma^2}{\mu}, \tag{4}$$

with $\sigma^2 = \mathrm{E}\left[\|\langle \nabla L_{\theta^*} \rangle\|^2\right] - \overbrace{\mathrm{E}[\|\langle \nabla L_{\theta^*} \rangle\|]^2}^{=0}$ and it's value depends on the choice of norm. The expected value of the gradient norm is zero for the optimal set of parameters θ^*, as the solution of the gradient descent is reached when the gradient converges to zero. This equation underscores the significance of minimizing variance in gradient estimation to enhance the convergence rate of gradient descent methods. While not universally applicable, it provides valuable insights into expected behavior when reducing estimation errors. Hence, refining gradient estimates is crucial for optimizing various learning algorithms, facili-

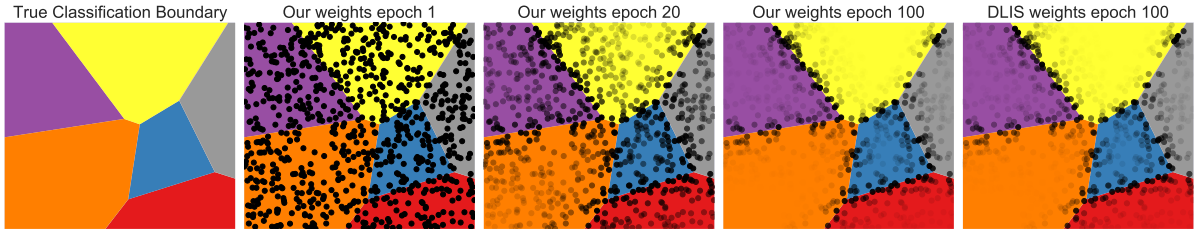


Figure 1: Visualization of the importance sampling at 3 different epoch and the underlying classification task. For each presented epoch, 800 data-point are presented with a transparency proportional to their weight according to our method. At epoch 800 our weights show high similarity to DLIS method while in practice some discrepancy differentiate the two method but are not visible in this simple example.

tating more efficient convergence towards optimal solutions. Our experimental evaluation comparing different methods in Section 4.2 further supports this notion.

4 Importance function

4.1 Gradient norm bound

The gradient L_2 norm has been shown to be an optimal choice of importance sampling (Zhao and Zhang, 2015; Needell et al., 2014; Wang et al., 2017; Alain et al., 2015) as it minimizes the first term of the gradient variance, thereby bounding the convergence of Eq. (4). However, calculating it requires costly full backpropagation for every data point, which is what we want to avoid in the first place. Instead, we compute an upper bound of the gradient L_2-norm using the output nodes of the network: $q(x) = \left\| \frac{\partial \mathcal{L}(x)}{\partial m(x,\theta)} \right\|$. This upper bound of the gradient norm is derived from the chain rule and the Cauchy–Schwarz inequality:

$$\left\| \frac{\partial \mathcal{L}(x_i)}{\partial \theta} \right\| = \left\| \frac{\partial \mathcal{L}(x)}{\partial m(x,\theta)} \cdot \frac{\partial m(x,\theta)}{\partial \theta} \right\| \tag{5}$$
$$\leq \left\| \frac{\partial \mathcal{L}(x)}{\partial m(x,\theta)} \right\| \cdot \left\| \frac{\partial m(x,\theta)}{\partial \theta} \right\| \leq \underbrace{\left\| \frac{\partial \mathcal{L}(x)}{\partial m(x,\theta)} \right\|}_{q(x)} \cdot C,$$

where C is the Lipschitz constant of the parameters gradient. That is, our importance function is a bound of the gradient magnitude based on the output-layer gradient norm. For specific shapes of the output layer, it is possible to derive a closed form expression. Below we show such derivation for classification networks based on the cross-entropy loss.

Cross-entropy loss gradient. Cross entropy is the standard loss function in classification tasks. It quantifies the dissimilarity between predicted probability distributions and actual class labels. Specifically, for a multi-class classification task, cross entropy is defined as:

$$\mathcal{L}(m(x_i,\theta)) = -\sum_{j=1}^{J} y_j \log(s_j)$$
$$\text{where } s_j = \frac{\exp(m(x_i,\theta)_j)}{\sum_{k=1}^{J} \exp(m(x_i,\theta)_k)} \tag{6}$$

where $m(x_i,\theta)$ is an output layer, x_i is the input data and J means the number of classes. It is possible to express the derivative of the loss $\mathcal{L}$ with respect to the network output $m(x_i,\theta)_j$ in a close form.

$$\frac{\partial \mathcal{L}}{\partial m(x_i,\theta)_j} = s_j - y_j \tag{7}$$

This equation can be directly computed from the network output without any graph back-propagation. This make the computation of our importance function extremely cheap for classification tasks. Proof of the derivation can be found in the Appendix A.

Importance sampling in classification emphasizes gradients along classification boundaries, where parameter modifications have the greatest impact. Figure 1 illustrates this concept, showing iterative refinement of the sampling distribution to focus on boundary decisions in comparison to data within classes. The rightmost column illustrates the sampling distribution of the DLIS method of Katharopoulos and Fleuret (2018) at epoch 100. Both methods iteratively increase the importance of the sampling around the boundary decision compare to data inside the classes.

Our approach differs from that of Katharopoulos and Fleuret in that we compute the gradient norm with respect to the network's output logits. This approach often allows gradient computation without requiring back-propagation or graph computations, streamlining optimization.

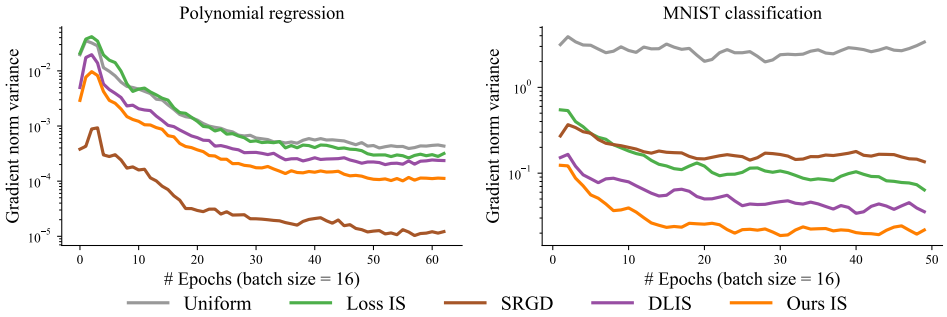


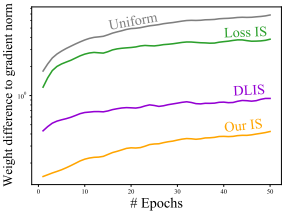
Figure 2: Evolution of gradient variance for variance importance sampling strategies on polynomial regression and MNIST classification task. In both case the optimization is done on a 3 fully-connected layer network. Variance estimation is made of each method on the same network at each epoch. The variance is computed using a mini-batch of size 16. Computation time for each metric can be found in Appendix D Table 2

4.2 Convergence analysis

Building on the theoretical bound defined in Eq. (4), we proceed to examine the effects of various importance sampling methods on the gradient variance. Such variance influences the convergence of an optimization procedure. This equation relies on the ideal model parameters θ^*, but they cannot be practically calculated. Rather, we measure the gradient variance during training using a suboptimal parameter set.

Figure 2 displays the evolution of gradient variance using different strategies for polynomial regression and MNIST classification, both using a three-layer fully connected network. Each method is evaluated on the same network, trained using uniform sampling. This allows for a variances comparison of the gradient norm. We analyze five techniques: Uniform sampling, Loss-based importance sampling, SRGD (Hanchi et al., 2022), DLIS (Katharopoulos and Fleuret, 2018), and our method. SRGD is an importance sampling technique using a conditioned minimization of gradient variance using memory of the gradient magnitude. This method has shown robust theoretical convergence properties in strongly convex scenarios. This variance reduction is visible on the polynomial regression task where it result in lower variance than other methods. However, for more complex tasks such as MNIST classification, SRGD underperforms all methods, suggesting scalability limitations to non-convex and complex problems. In contrast, our method consistently yields lower variance than Loss-based importance sampling and DLIS (Katharopoulos and Fleuret, 2018). These findings elucidate the results in Section 7.

In addition, we provide evaluation times for each metric for both the polynomial regression and MNIST classification tasks in Appendix D Table 2. Clearly, SRGD (Hanchi et al., 2022) demands more computational resources, even for small-scale networks comprising only three layers. This increased demand stems from its dependence on calculating the gradient norm for each individual data point. Both our metric, which employs automatic differentiation, and DLIS (Katharopoulos and Fleuret, 2018), incur comparable computational costs due to their reliance on derivatives from the final layers. Nonetheless, our approach proves to be the most efficient when analytical evaluations are feasible. Such differences in computational efficiency are likely to significantly influence the outcomes of comparisons made under equal-time conditions in later sections.



Zhao and Zhang (2015) have shown that importance weights w.r.t. the gradient norm gives the optimal sampling distribution. On the right inline figure, we show the difference between various weighting strategies and the gradient norm w.r.t. all parameters. In this experiment, all sampling weights are computed using the same network on an MNIST optimization task. Our proposed sampling strategies, based on the loss gradient are the closest approximation to the gradient norm.

5 Online importance sampling algorithm

We propose an algorithm to efficiently perform importance sampling for mini-batch gradient descent, outlined in Algorithm 1. Similarly to Loshchilov and Hutter (2015) and Schaul et al. (2015), it is designed

to use an importance function that relies on readily available quantities for each data point, introducing only negligible memory and computational overhead over classical uniform mini-batching.

Algorithm 1 Mini-batch importance sampling for SGD.

1: $\theta \leftarrow$ random parameter initialization
2: $B \leftarrow$ mini-batch size, $N = |\Omega|$ ← Dataset size
3: $q, \theta \leftarrow \text{Initialize}(\Omega, \theta, B)$ ← Algorithm 3
4: **until** convergence **do** ← Loop over epochs
5: **for** $t \leftarrow 1$ **to** N/B ← Loop over mini-batches
6: $p \leftarrow q/\text{sum}(q)$ ← Normalize importance to pdf
7: $x, y \leftarrow B$ data samples $\{x_i, y_i\}_{i=1}^{B} \propto p$
8: $\mathcal{L}(x) \leftarrow \mathcal{L}(m(x, \theta), y)$
9: $\nabla\mathcal{L}(x) \leftarrow \text{Backpropagate}(\mathcal{L}(x))$
10: $\langle \nabla L_\theta \rangle \leftarrow (\nabla\mathcal{L}(x) \cdot (1/p(x))^T)/B$ ← Eq. (3)
11: $\theta \leftarrow \theta - \eta \langle \nabla L_\theta \rangle$ ← SGD step
12: $q(x) \leftarrow \alpha \cdot q(x) + (1-\alpha) \cdot \left\| \frac{\partial \mathcal{L}(x)}{\partial m(x,\theta)} \right\|$
13: ↳ Accumulate importance
14:
15: $q \leftarrow q + \varepsilon$
16: ↳ to ensures no data samples are forgotten indefinitely
17: **return** θ

We maintain a set of persistent *un-normalized importance* scalars $q = q_i|_{i=1}^{|\Omega|}$, continually updated during optimization. Initially, we process all data points once in the first epoch to determine their initial importance (line 3). Subsequently, at each mini-batch optimization step t, we normalize the importance values to obtain the probability density function (PDF) p (line 6), and use it to sample B data points with replacement (line 7). We then evaluate the loss for each selected data sample (line 8) and backpropagate to compute the corresponding loss gradient (line 9). Finally, we update the network parameters using the estimated gradient (line 11). Additionally, we compute the sample importance for each data sample from the mini-batch and update the persistent importance q (line 12). Various importance heuristics such as the gradient norm (Zhao and Zhang, 2015; Needell et al., 2014; Wang et al., 2017; Alain et al., 2015), the loss (Loshchilov and Hutter, 2015; Katharopoulos and Fleuret, 2017; Dong et al., 2021) or more advanced importance (Katharopoulos and Fleuret, 2018) can be implemented to replace our sampling metric in this line. To enhance efficiency, our algorithm reuses the forward pass computations made during line 8 to compute importance, updating q only for the current mini-batch samples. The weighting parameter α ensures weight stability as discussed in Eq. (8).
At the end of each epoch (line 15), we add a small value to the un-normalized weights of all data to ensure that every data point will be eventually evaluated, even if its importance is deemed low by the importance metric.

It is importance to note that the initialization epoch is done without importance sampling to initialize each sample importance. This does not create overhead as it is equivalent to a classical epoch running over all data samples. While similar schemes have been proposed in the past, they often rely on a multitude of hyperparameters, making their practical implementation challenging. This has led to the development of alternative methods like re-sampling (Katharopoulos and Fleuret, 2018; Dong et al., 2021; Zhang et al., 2023). Our proposed sampling strategy has only a few hyperparameters. Tracking importance across batches and epochs minimizes the computational overhead, further enhancing the efficiency and practicality of the approach.

6 Online data pruning

Data pruning is a technique aimed at reducing the size of the dataset to accelerate training. The acceleration can be attributed to two main factors. The first, and most practical, relates to the execution speed of training neural networks. When working with large datasets, especially those with a relatively large memory footprint, it is often infeasible to store all data directly in GPU memory. This necessitates frequent data loading from slower storage mediums, which can become a bottleneck and significantly slow down training. By reducing the dataset size, less data needs to be loaded during each training iteration, leading to faster execution, even if the theoretical properties of the training process remain unchanged. The second factor contributing to faster training is theoretical. If the pruned data points have a low gradient norm, removing them increases the expected gradient norm of the remaining data points. This, in turn, leads to larger effective steps in the optimization process, thus accelerating convergence.

Given these two benefits, we propose a data pruning strategy guided by our novel importance metric, which serves as an estimate of the gradient norm for each data point. Unlike most previous works that rely on precomputed metrics or early-stage proxies, our metric is adaptive throughout training and does not require any precomputation. This allows us to dynamically prune the dataset based on current information about the importance of each data point.

Our approach involves an online pruning process that operates as follows: After a certain number of

Table 1: We compare the impact of our importance sampling algorithm with or without data pruning on classification tasks. We compare on three different datasets: Point cloud, CIFAR-100 and Tiny-ImageNet. Our approach consistently outperform on majority of datasets (see Table 3 for more comparisons). Bold numbers represents the best scores, underlined ones represent the second best.

	Point cloud				**CIFAR-100**				**Tiny-ImageNet**			
	Equal step		**Equal time**		**Equal step**		**Equal time**		**Equal step**		**Equal time**	
Method	**Loss (↓)**	**Accuracy (↑)**	**Loss**	**Accuracy**	**Loss**	**Accuracy**	**Loss**	**Accuracy**	**Loss**	**Accuracy**	**Loss**	**Accuracy**
Uniform	0.00505	82.3	0.00505	82.2	0.012	72.6	0.012	73.8	<u>0.02176</u>	<u>47.4</u>	<u>0.02176</u>	<u>47.4</u>
Loss IS	0.00495	82.6	0.00496	82.5	0.023	40.2	0.026	32.8	0.02237	45.2	0.02238	45.2
DLIS	0.00595	81.9	0.00603	81.8	0.015	62.0	0.015	60.8	0.03433	26.3	0.03433	26.3
DLIS weights **w/ Our algorithm**	0.00481	82.6	0.00485	82.5	0.021	43.6	0.029	26.3	0.03454	26.1	0.02778	35.0
LOW	0.00572	82.6	0.01173	74.9	<u>0.011</u>	**74.6**	<u>0.011</u>	74.2	0.02344	43.5	0.02344	43.5
Our IS	<u>0.00480</u>	<u>82.9</u>	<u>0.00480</u>	<u>82.9</u>	0.011	74.3	0.012	<u>74.3</u>	**0.02127**	**48.1**	**0.02123**	**48.5**
Our IS + Data pruning	**0.00478**	**83.2**	**0.00478**	**83.1**	**0.011**	<u>74.3</u>	**0.011**	**74.3**	0.02193	47.1	0.02193	47.1

Algorithm 2 Subroutine for data pruning

function ONLINEDATAPRUNING(Ω,q,K,ε)
  $\varepsilon \leftarrow \frac{1}{K|\Omega|}\sum_{x\in\Omega} q(x)$ ← Compute pruning threshold
  $\Omega' \leftarrow \Omega_{\{q(x)>\varepsilon|\forall x\in\Omega\}}$
  return Ω' ↳ Filter dataset to keep high importance data

epochs, we ensure that the importance metric has been calculated for all data points in the training set. At this point, we identify and remove a portion of the data with importance metrics significantly lower than the average. Specifically, each data point's importance is compared to the average importance across the dataset. If a data point's importance falls below a threshold relative to the average, it is pruned from the training set. This ensures that only data points with low expected gradient norms are removed, while important data remains. Algorithm 2 depicts the pruning subroutine, which processes the dataset Ω, the importance score for each data point q, and a reduction factor K. A higher reduction factor results in retaining more data points, thus fewer data are pruned.

This process is flexible and can adapt to the distribution of importance values in the dataset. If the dataset has a wide distribution of importance, with only a few data points contributing significantly to the optimization, a large portion of the dataset can be pruned. Conversely, if all data points exhibit relatively high importance, few or no data points will be removed. Furthermore, since our importance metric is adaptive, this pruning process can be applied multiple times throughout training. By continually updating the importance metric and pruning low-importance data points, we maintain an efficient training set that accelerates the learning process without compromising model performance.

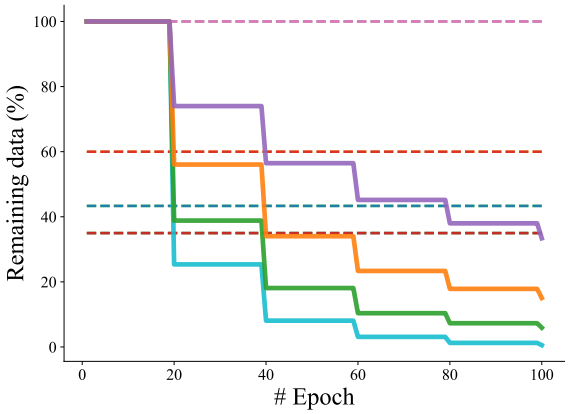
7 Experiments

In this section, we delve into the experimental outcomes of our proposed algorithm and sampling strategy. Our evaluations encompass diverse classification and regression tasks. We benchmarked our approach against those of Katharopoulos and Fleuret (2018) and Santiago et al. (2021), considering various variations in comparison. Distinctions in our comparisons lie in assessing performance at equal steps/epochs and equal time intervals. The results presented here demonstrate the loss and classification error, computed on test data that remained unseen during the training process.

7.1 Implementation details

We implement our method and all baselines in a single PyTorch framework. Experiments run on a workstation with an NVIDIA Tesla A40 graphics card. The baselines include uniform sampling, DLIS (Katharopoulos and Fleuret, 2018) and LOW (Santiago et al., 2021). Uniform means that we sample every data point from a uniform distribution. DLIS importance samples the data mainly depending on the norm of the gradient on the last output layer. We use functorch (Horace He, 2021) to accelerate this gradient computation. LOW is based on adaptive weighting that maximizes the effective gradient of the mini-batch using the solver from Vandenberghe (2010).

We evaluated our method on a range of tasks, including image classification with MNIST, CIFAR-10/100 (Krizhevsky et al., 2009), Tiny-ImageNet (Le and Yang, 2015), and Oxford Flower-102 (Nilsback and Zisserman, 2008), as well as Point cloud classification (Qi et al., 2017) and regression tasks (Sitzmann et al., 2020). Full details on the datasets used, along with optimization parameters such as learning rate, optimizer scheduler and the data pruning ratio



Method	Accuracy	Remaining data (At end of opt.)	Training time(s) (Pruning time)
Uniform	96.4%	100%	554 (0)
Random pruning	96.3%	60%	131 (3)
Random pruning	96.2%	43%	121 (2)
Random pruning	96.1%	35%	114 (1)
Yang et al. (2023)	96.4%	60%	132 (2388)
Yang et al. (2023)	96.3%	43%	128 (4825)
Yang et al. (2023)	96.2%	35%	121 (9351)
Ours (K=8)	97.9%	62% (33%)	215 (3)
Ours (K=4)	98.1%	45% (15%)	214 (2)
Ours (K=2)	98.1%	34% (6%)	208 (2)
Ours (K=1)	92.6%	27%(0.6%)	203 (2)

Figure 3: Evaluation of the impact of the amount of data pruned during training on a MNIST classification task. The left panel shows the evolution of the pruned data over time, while the right panel presents the final accuracy, the average training set size during training and remaining data at the end of training, the total training time, and the computation time of pruning. The figure compares a uniform sampling without data pruning, random pruning with 60%, 43%, and 35% of data pruned, the method of Yang et al. (2023) at the same pruning rates, and our approach using a dynamic reduction factor K. Results indicate that pruning more data accelerates execution. Our online pruning method offers greater adaptability during training while maintaining high accuracy and minimal difference between training time and total execution time.

and frequency are provided in Appendix C. In all results involving pruning, the number of steps per epoch remains consistent with the non-pruned experiments. This ensures a fair comparison at equal steps, meaning that with pruning, certain data points are seen multiple times within each epoch to match the total step count.

Weight stability. Updating the persistent per-sample importance q directly sometime leads to a sudden decrease of accuracy during training. To make the training process more stable, we update q by linearly interpolating the importance at the previous and current steps:

$$q(x) = \alpha \cdot q_{prev}(x) + (1-\alpha) \cdot q(x) \tag{8}$$

where α is a constant for all data samples. In practice, we use $\alpha \in \{0.0, 0.1, 0.2, 0.3\}$ as it gives the best trade-off between importance update and stability. This can be seen as a momentum evolution of the per-sample importance to avoid high variation. Utilizing an exponential moving average to update the importance metric prevents the incorporation of outlier values. This is particularly beneficial in noisy setups, like situations with a high number of class or a low total number of data. Details on the chosen α values can be found in Appendix C.

7.2 Results

In Table 1, we compare Uniform sampling, Loss-based importance sampling, the method from Katharopoulos and Fleuret (2018) and their weights in our algorithm, the approach from Santiago et al. (2021), and our method with both importance sampling and data pruning. The table reports the cross-entropy loss and classification accuracy for three tasks: point cloud classification, CIFAR-100, and Tiny-ImageNet. Results are shown for both an equal number of steps and equal runtime. The best results are highlighted in bold, with the second-best underlined. Across all three tasks, our method consistently achieves the best performance in both scenarios. Even in cases where importance sampling offers minimal improvement, our approach proves more robust than DLIS and LOW, avoiding significant underperformance in challenging situations. In the Tiny-ImageNet experiment, although data pruning results in a slight drop in accuracy, the outcome aligns with the observations from Yang et al. (2023), where pruning can leads to a small reduction in generalization. Additional results on other datasets can be found in Table 3.

Figure 4 illustrates the results of a regression task on an image using a SIREN network to learns the mapping between 2D pixel coordinates and the corresponding RGB color. The left panel shows the loss evolution for all methods, while the right panel

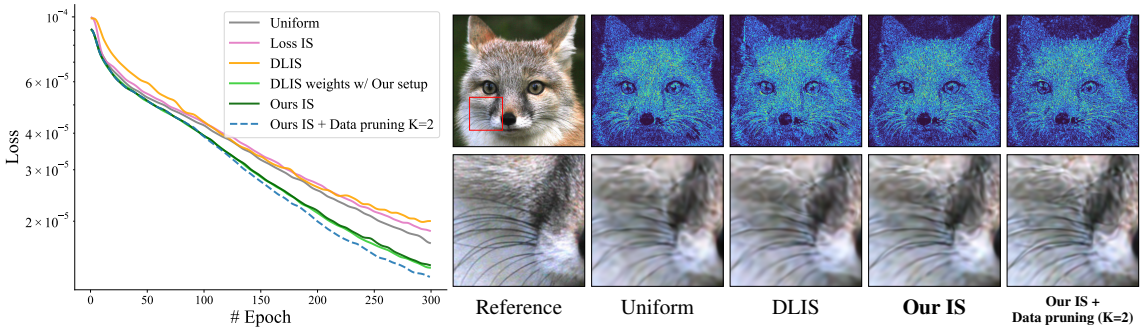


Figure 4: Comparison at equal step for image 2D regression. The left side shows the convergence plot while the right display the absolute error of the regression and a close-up view. Our method using data pruning achieves the lower error on this problem while pruning 45% of the data during training. Our method using only importance sampling and DLIS with our algorithm perform similarly, but DLIS with their full method perform worse than default optimization. In the images it is visible that our method with pruning recovers the finest details of the fur and whiskers.

presents the error maps at final steps, along with a zoomed-in region for Uniform sampling, DLIS, our method with importance sampling, and our method combining importance sampling and data pruning. Our method, which incorporates importance sampling and data pruning, provides the best loss reduction performance. The error map reveals fewer errors, with less yellow tones and finer details in the zoomed region. This method effectively reduces error in high-frequency regions by compensating in smoother regions such as the background, leading to a more balanced error distribution across the image. In comparison, DLIS produces similar results to our importance sampling when its weights are used with our algorithm, but its full method is significantly outperformed by Uniform sampling. This is evident in the error map and the zoomed-in area, which display more blurriness in DLIS results.

Figure 3 presents an ablation study of our online pruning strategy on the MNIST classification task, comparing random pruning, the method of Yang et al. (2023), and our adaptive approach. The left side shows the evolution of the data used during training across epochs, while the right side highlights final accuracy, the average data used per epoch and the final remaining data, the training time and time used to compute the pruning. Our adaptive method starts with the full dataset and prunes data every 20 epochs, following Algorithm 2. As training progresses, the amount of pruned data decreases, since many data points begin to contribute redundant information. By the end, only a reduced subset remains. In contrast, Yang et al. (2023) prunes in one step at the start using a pre-trained model, leading to faster training but lower quality results, not outperforming uniform sampling but providing generalization properties. Our approach adaptively removes data that no longer adds value to the learning process. While aggressive pruning (e.g., $K = 1$) risks overfitting and reduced accuracy, more moderate pruning speeds up training without sacrificing quality. The results show that when minimal or no pruning is applied, the advantages diminish, reverting to a reliance on importance sampling alone. Overall, our adaptive pruning efficiently reduces dataset size while preserving crucial data throughout training.

Additional experiments. Further comparisons, similar to those in Table 1, across various datasets are provided in Appendix D. We also present convergence curves at equal steps and equal time intervals for Pointnet, CIFAR-10 (ViT (Dosovitskiy et al., 2021)) and Tiny-ImageNet, demonstrating the consistent improvements of our method throughout the optimization process. These additional experiments reinforce the effectiveness of our approach and in particular benefit from a low computation method at equal time.

Discussion. Both our and DLIS importance metrics are highly correlated, but ours is simpler and more efficient to evaluate. Even with a slightly better importance sampling metric, most of the improvement come from the memory-based algorithm instead of a resampling one. The resulting algorithm gives better performance at the same time and has more stable convergence. Our online data pruning method is controlled by a pruning factor K, which dictates how much data is removed at each step. While we kept K constant in our experiments, it could be adjusted to prevent overfitting. Pruned data could also be reintroduced later to check for overfitting by observing if its importance increases after removal. This could help detect reduced generalization without shrinking the initial dataset, though we leave this for future work.

In theory, importance sampling can achieve error-free estimation, when the sampling distribution is exactly proportional to the integrand. However, that theoretical property holds only in the case where the estimated quantity is scalar. In our case error-free estimation is impossible even theoretically, because the estimated gradient is multi-dimensional, and there does not exist a single (scalar) distribution that is proportional to each dimension (i.e., parameter derivative). To address this issue, Salaün et al. (2024) explore the use of multiple sampling distributions to further enhance gradient estimation. Their method builds upon similar sampling metrics and algorithms to those proposed in this paper, demonstrating the potential for improved accuracy through the use of diverse sampling strategies.

Limitations. As the algorithm rely on past information to drive a non-uniform sampling of data, it requires seeing the same data multiple times. This creates a bottleneck for architectures that rely on progressive data streaming. More research is needed to design importance sampling algorithms for data streaming architectures, which is a promising future direction. Non-uniform data sampling can also create slower runtime execution. The samples selected in a mini-batch are not laid out contiguously in memory leading to a slower loading. We believe a careful implementation can mitigate this issue.

8 Conclusion

In conclusion, our work introduces an efficient sampling strategy for machine learning optimization, that can be use for importance sampling and data pruning. This strategy, which relies on the gradient of the loss and has minimal computational overhead, was tested across various classification as well as regression tasks with promising results. Our work demonstrates that by paying more attention to samples with critical training information, we can speed up convergence without adding complexity. We hope our findings will encourage further research into simpler and more effective sampling strategies for machine learning.

REFERENCES

Alain, G., Lamb, A., Sankar, C., Courville, A., and Bengio, Y. (2015). Variance reduction in sgd by distributed importance sampling. *arXiv preprint arXiv:1511.06481*.

Bordes, A., Ertekin, S., Weston, J., and Bottou, L. (2005). Fast kernel classifiers with online and active learning. *Journal of Machine Learning Research*, 6(54):1579–1619.

Coleman, C., Yeh, C., Mussmann, S., Mirzasoleiman, B., Bailis, P., Liang, P., Leskovec, J., and Zaharia, M. (2020). Selection via proxy: Efficient data selection for deep learning. In *International Conference on Learning Representations*.

Dong, C., Jin, X., Gao, W., Wang, Y., Zhang, H., Wu, X., Yang, J., and Liu, X. (2021). One backward from ten forward, subsampling for large-scale deep learning. *arXiv preprint arXiv:2104.13114*.

Dosovitskiy, A., Beyer, L., Kolesnikov, A., Weissenborn, D., Zhai, X., Unterthiner, T., Dehghani, M., Minderer, M., Heigold, G., Gelly, S., Uszkoreit, J., and Houlsby, N. (2021). An image is worth 16x16 words: Transformers for image recognition at scale. In *International Conference on Learning Representations*.

Faghri, F., Duvenaud, D., Fleet, D. J., and Ba, J. (2020). A study of gradient variance in deep learning. *arXiv preprint arXiv:2007.04532*.

Gower, R. M., Loizou, N., Qian, X., Sailanbayev, A., Shulgin, E., and Richtárik, P. (2019). SGD: General analysis and improved rates. In Chaudhuri, K. and Salakhutdinov, R., editors, *Proceedings of the 36th International Conference on Machine Learning*, volume 97 of *Proceedings of Machine Learning Research*, pages 5200–5209. PMLR.

Gower, R. M., Schmidt, M., Bach, F., and Richtárik, P. (2020). Variance-reduced methods for machine learning. *Proceedings of the IEEE*, 108(11):1968–1983.

Hanchi, A. E., Stephens, D., and Maddison, C. (2022). Stochastic reweighted gradient descent. In Chaudhuri, K., Jegelka, S., Song, L., Szepesvari, C., Niu, G., and Sabato, S., editors, *Proceedings of the 39th International Conference on Machine Learning*, volume 162 of *Proceedings of Machine Learning Research*, pages 8359–8374. PMLR.

Har-Peled, S. and Kushal, A. (2005). Smaller coresets for k-median and k-means clustering. In *Proceedings of the Twenty-First Annual Symposium on Computational Geometry*, SCG '05, page 126–134, New York, NY, USA. Association for Computing Machinery.

He, K., Zhang, X., Ren, S., and Sun, J. (2016). Deep residual learning for image recognition. In *Proceedings of the IEEE conference on computer vision and pattern recognition*, pages 770–778.

Horace He, R. Z. (2021). functorch: Jax-like composable function transforms for pytorch. https://github.com/pytorch/functorch.

Johnson, R. and Zhang, T. (2013). Accelerating stochastic gradient descent using predictive variance reduction. *Advances in neural information processing systems*, 26.

Katharopoulos, A. and Fleuret, F. (2017). Biased importance sampling for deep neural network training. *ArXiv*, abs/1706.00043.

Katharopoulos, A. and Fleuret, F. (2018). Not all samples are created equal: Deep learning with importance sampling. In Dy, J. and Krause, A., editors, *Proceedings of the 35th International Conference on Machine Learning*, volume 80 of *Proceedings of Machine Learning Research*, pages 2525–2534. PMLR.

Kingma, D. P. and Ba, J. (2014). Adam: A method for stochastic optimization. *arXiv preprint arXiv:1412.6980*.

Krizhevsky, A., Hinton, G., et al. (2009). Learning multiple layers of features from tiny images.

Le, Y. and Yang, X. (2015). Tiny imagenet visual recognition challenge. *CS 231N*, 7(7):3.

Loshchilov, I. and Hutter, F. (2015). Online batch selection for faster training of neural networks. *arXiv preprint arXiv:1511.06343*.

Needell, D., Ward, R., and Srebro, N. (2014). Stochastic gradient descent, weighted sampling, and the randomized kaczmarz algorithm. In Ghahramani, Z., Welling, M., Cortes, C., Lawrence, N., and Weinberger, K., editors, *Advances in Neural Information Processing Systems*, volume 27. Curran Associates, Inc.

Nilsback, M.-E. and Zisserman, A. (2008). Automated flower classification over a large number of classes. In *2008 Sixth Indian conference on computer vision, graphics & image processing*, pages 722–729. IEEE.

Paul, M., Ganguli, S., and Dziugaite, G. K. (2021). Deep learning on a data diet: Finding important examples early in training. *Advances in neural information processing systems*, 34:20596–20607.

Qi, C. R., Su, H., Mo, K., and Guibas, L. J. (2017). Pointnet: Deep learning on point sets for 3d classification and segmentation. In *Proceedings of the IEEE conference on computer vision and pattern recognition*, pages 652–660.

Qin, Z., Wang, K., Zheng, Z., Gu, J., Peng, X., Xu, Z., Zhou, D., Shang, L., Sun, B., Xie, X., and You, Y. (2023). Infobatch: Lossless training speed up by unbiased dynamic data pruning.

Salaün, C., Huang, X., Georgiev, I., Mitra, N. J., and Singh, G. (2024). Multiple importance sampling for stochastic gradient estimation. *arXiv preprint arXiv:2407.15525*.

Santiago, C., Barata, C., Sasdelli, M., Carneiro, G., and Nascimento, J. C. (2021). Low: Training deep neural networks by learning optimal sample weights. *Pattern Recognition*, 110:107585.

Schaul, T., Quan, J., Antonoglou, I., and Silver, D. (2015). Prioritized experience replay. *arXiv preprint arXiv:1511.05952*.

Simonyan, K. and Zisserman, A. (2014). Very deep convolutional networks for large-scale image recognition. *arXiv preprint arXiv:1409.1556*.

Sitzmann, V., Martel, J., Bergman, A., Lindell, D., and Wetzstein, G. (2020). Implicit neural representations with periodic activation functions. *Advances in neural information processing systems*, 33:7462–7473.

Toneva, M., Sordoni, A., des Combes, R. T., Trischler, A., Bengio, Y., and Gordon, G. J. (2019). An empirical study of example forgetting during deep neural network learning. In *International Conference on Learning Representations*.

Vandenberghe, L. (2010). The cvxopt linear and quadratic cone program solvers. *Online: http://cvxopt. org/documentation/coneprog. pdf*.

Wang, L., Yang, Y., Min, R., and Chakradhar, S. (2017). Accelerating deep neural network training with inconsistent stochastic gradient descent. *Neural Networks*, 93:219–229.

Wu, Z., Song, S., Khosla, A., Yu, F., Zhang, L., Tang, X., and Xiao, J. (2015). 3d shapenets: A deep representation for volumetric shapes. In *Proceedings of the IEEE conference on computer vision and pattern recognition*, pages 1912–1920.

Yang, S., Xie, Z., Peng, H., Xu, M., Sun, M., and Li, P. (2023). Dataset pruning: Reducing training data by examining generalization influence. In *The Eleventh International Conference on Learning Representations*.

Zhang, C., Kjellstrom, H., and Mandt, S. (2017). Determinantal point processes for mini-batch diversification. *arXiv preprint arXiv:1705.00607*.

Zhang, C., Öztireli, C., Mandt, S., and Salvi, G. (2019). Active mini-batch sampling using repulsive point processes. In *Proceedings of the AAAI conference on Artificial Intelligence*, volume 33, pages 5741–5748.

Zhang, M., Dong, C., Fu, J., Zhou, T., Liang, J., Liu, J., Liu, B., Momma, M., Wang, B., Gao, Y., et al. (2023). Adaselection: Accelerating deep learning training through data subsampling. *arXiv preprint arXiv:2306.10728*.

Zhao, P. and Zhang, T. (2015). Stochastic optimization with importance sampling for regularized loss minimization. In Bach, F. and Blei, D., editors, *Proceedings of the 32nd International Conference on Machine Learning*, volume 37 of *Proceedings of Machine Learning Research*, pages 1–9, Lille, France. PMLR.

A Derivative of cross-entropy loss

Machine learning frameworks take data x as input, performs matrix multiplication with weights and biases added. The output layer is then fed to the softmax function to obtain values s that are fed to the loss function. y represents the target values (a series of zeros for incorrect classes and one for the correct class). The softmax layer at the end of the classifier guarantees that the total of the outputs equals one. We focus on the categorical cross-entropy loss function for the classification problem (with J categories) given by:

$$\mathcal{L}_{\text{cross-ent}} = -\sum_i y_i \log s_i \quad \text{where } s_i = \frac{\exp(m(x_i,\theta)_l)}{\sum_l^J \exp(m(x_i,\theta)_l)} \tag{9}$$

For backpropagation, we need to calculate the derivative of the $\log s$ term wrt the weighted input z of the output layer. We can easily derive the derivative of the loss from first principles as shown below:

$$\frac{\partial \mathcal{L}_{\text{cross-ent}}}{\partial m(x_i,\theta)_j} = -\frac{\partial}{\partial m(x_i,\theta)_j}\left(\sum_i^J y_i \log s_i\right) \tag{10}$$

$$= -\sum_i^J y_i \frac{\partial}{\partial m(x_i,\theta)_j} \log s_i \tag{11}$$

$$= -\sum_i^J \frac{y_i}{s_i} \frac{\partial s_i}{\partial m(x_i,\theta)_j} \tag{12}$$

$$= -\sum_i^J \frac{y_i}{s_i} s_i \cdot (\mathbf{1}\{i == j\} - s_j) \tag{13}$$

$$= \sum_i^J y_i \cdot s_j - \sum_i^J y_i \cdot (\mathbf{1}\{i == j\}) \tag{14}$$

$$= s_j \sum_i^J y_i - y_j = s_j - y_j \tag{15}$$

The partial derivative of the cross-entropy loss function wrt output layer parameters has the form:

$$\frac{\partial \mathcal{L}_{\text{cross-ent}}}{\partial m(x_i,\theta)_j} = s_j - y_j \tag{16}$$

For classification tasks, we directly use this analytic form of the derivative and compute it's norm as weights for importance sampling.

B Algorithm details

Algorithm 3 provide detail on the initialization subroutine applying a first epoch of training without importance sampling to initialize the persistent importance vector q.

C Dataset and training details

In this section we provide details of the datasets and training. We train all models with 3 independent runs and report the average loss and accuracy as shown in Table 3.

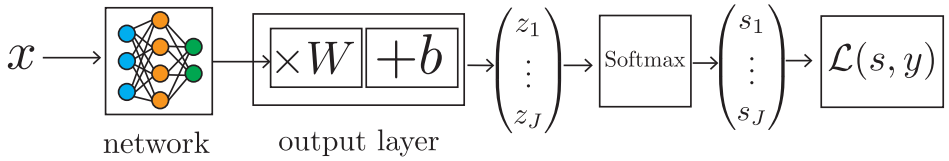
MNIST. The MNIST database contains 60,000 training images and 10,000 testing images. We train a 3-layer fully-connected network (MLP) for image classification over 50 epochs with an Adam optimizer (Kingma and Ba, 2014).

CIFAR-10 and CIFAR-100. CIFAR-10 (Krizhevsky et al., 2009) contains 60,000 32x32 color images from 10 different object classes, with 6,000 images per class. CIFAR-100 (Krizhevsky et al., 2009) has 100 classes containing 600 images each, with 500 training images and 100 testing images per class. For both datasets, we use the ResNet-18 network architecture (He et al., 2016). We use the SGD optimizer with momentum 0.9, initial leaning rate 0.003 (CIFAR-10) and 0.007 (CIFAR-100), and batch size 128. We reduced the initial learning rate following an exponential scheduling with factor 0.987 over a total of 120 epochs for CIFAR-10 and 200 epochs for CIFAR-100. For both datasets, we use random horizontal flip, random crops to augment the data on the fly and use We used $\alpha = 0.3$ for the importance memory update and $K = 4$ for the pruning factor.

For CIFAR-10, we also trained a Vision Transformer (ViT) (Dosovitskiy et al., 2021) using the Adam optimizer with an initial learning rate 0.0001, divided by 10 after 70, 140 epochs. Here we also use random horizontal flip, random crops to augment the data on the fly and use $\alpha = 0.3$ for the importance memory update and $K = 8$ for the pruning factor.

Point-cloud classification. We train a PointNet (Qi et al., 2017) with 3 shared-MLP layers and one fully-connected layer, on the ModelNet40 dataset (Wu et al., 2015). The dataset contains point clouds from 40 categories, with 1,024 points each. The data are split into 9,843 for training and 2,468 for testing. We use the Adam optimizer with batch size 64, weight decay 0.001, initial learning rate 0.00002 divided by 10 after 100, 200 epochs. We train for 300 epochs in total We used $\alpha = 0.0$ and $K = 8$ for our methods.

Oxford Flower-102. The Oxford 102 flower dataset (Nilsback and Zisserman, 2008) contains flower images from 102 categories. We follow



Algorithm 3 Subroutine for initialization for Algorithm 1

function INITIALIZE(Ω,θ,B)
  for $t \leftarrow 1$ **to** $|\Omega|/B$
    $x,y \leftarrow \{x_i,y_i\}_{i=(t-1)\cdot B+1}^{t\cdot B+1}$ ← See all samples in the first epoch
    $\mathcal{L}(x) \leftarrow \mathcal{L}(m(x,\theta),y)$
    $\nabla\mathcal{L}(x) \leftarrow \text{Backpropagate}(\mathcal{L}(x))$
    $\langle \nabla L_\theta \rangle(x) \leftarrow \nabla\mathcal{L}(x)/B$ ← Eq. (3)
    $\theta \leftarrow \theta - \eta \langle \nabla L_\theta \rangle(x)$ ← Eq. (2)
    $q(x) \leftarrow \left\| \frac{\partial \mathcal{L}(x)}{\partial m(x,\theta)} \right\|$ ← Initialize per sample importance

  return q,θ

the same experiment setting of Zhang et al. (2017, 2019). We use the original test set for training (6,149 images) and the original training set for testing (1,020 images). In terms of network architecture, we use the pre-trained VGG-16 network (Simonyan and Zisserman, 2014) for feature extraction and only train a two-layer fully-connected network from scratch for classification. We use the Adam optimizer with a learning rate 0.001 and train the two-layer fully-connected network for 100 epochs. We used $\alpha = 0.2$ and $K = 8$ for our methods.

Tiny-ImageNet. Tiny-ImageNet dataset is proposed by Le and Yang (2015). Tiny-ImageNet is a larger dataset contains 100,000 training examples from 200 categories. We train a ResNet-18 network (He et al., 2016) for 20 epochs with a batch size of 64, a learning rate of 0.001 divided by 10 after 10 epochs, SGD optimizer with momentum 0.9 and data augmentation of random horizontal flip. We used $\alpha = 0.3$ and $K = 64$ for our methods.

Image regression. The image regression task involves training a network to learn a 2D image signal, where each pixel is treated as an individual data point. The input to the network is the pixel's 2D coordinates, and the output is the corresponding RGB value for that pixel. We trained a 5-layer SIREN network (Sitzmann et al., 2020) for 300 epoch using sinusoidal encoding for the input coordinates, optimized with Adam at a learning rate of 0.0003 and a batch size of 512. For our method we used $\alpha = 0.3$ and $K = 2$.

D Additional Experiments

In this section we present additional experiments.

Table 2 presents the computation times for four different importance metrics used in Fig. 2. Our importance metric is nearly as fast as simply using the loss for classification tasks, thanks to its analytic form. When utilizing automatic differentiation, the computation time of our metric is comparable to DLIS, as both require backpropagation on the network output (for ours) or the last layer (for DLIS). The final method, SRGD, involves a significantly more costly metric evaluation.

Table 3 presents a comparison between various methods, including Uniform sampling, Loss-based importance sampling, DLIS, DLIS with our algorithm, LOW, our method using only importance sampling, and a combination of importance sampling with data pruning across multiple tasks. For each task, we report the cross-entropy loss and accuracy at both equal steps and equal time, alongside the total optimization time for each method. Overall, our method, which combines importance sampling and data pruning, achieves the best results in terms of both equal time and equal steps. Although it does not always yield the top result, it frequently ranks second or first. Some specific cases are worth highlighting. In the CIFAR-10 classification task using a ViT network, we observe longer training times for our method, even with data pruning. This is due to the overhead introduced by gradient backpropagation and the relatively low level of pruning. This overhead is also noticeable in both DLIS methods. In the image regression task, where each pixel is treated as a separate data point, the

memory footprint is low. Consequently, data pruning does not lead to sufficient time reduction to offset the overhead introduced by importance sampling and its computation, which results in Uniform sampling outperforming our method in terms of computation time. Additionally, there are instances where our method using only importance sampling outperforms the version with data pruning. This occurs in cases where significant data pruning negatively impacts generalization. For instance, in the Flower-102 dataset, each class contains only a few examples, so pruning too many data points directly compromises the model's training capacity, as each point carries critical information.

Finally, we present three convergence curves—showing both loss and accuracy—under equal time and equal steps for CIFAR-10 (ViT) (Fig. 5), Point Cloud (Fig. 6), and Tiny-ImageNet (Fig. 7) classification tasks. These curves illustrate the evolution of classification error across the methods used in Table 3. Our method consistently achieves superior performance throughout the training process. Additionally, the results highlight significant underperformance for certain methods, such as DLIS on Tiny-ImageNet and CIFAR-10 (ViT). The results also emphasize the substantial difference between equal steps and equal time for the LOW method, which suffers from a considerable overhead. Although LOW performs well under equal steps, it can perform worse than Uniform sampling when evaluated at equal time.

Table 2: Average computation time on 3 layer fully-connected network for multiple sampling metric the task from Fig. 2. Time is average over one epoch and computed on mini-batch of size 16.

Computation time (↓)	**Loss**	**SRGD**	**DLIS**	**Ours autodiff**	**Ours analytic**
Polynomial regression	$1.33 \cdot 10^{-4}$ (1.×)	$7.17 \cdot 10^{-4}$ (5.39×)	$4.38 \cdot 10^{-4}$ (3.29×)	$3.23 \cdot 10^{-4}$ (2.43×)	-
MNIST	$1.28 \cdot 10^{-4}$ (1.×)	$5.57 \cdot 10^{-4}$ (4.35×)	$3.27 \cdot 10^{-4}$ (2.55×)	$3.59 \cdot 10^{-4}$ (2.80×)	$1.40 \cdot 10^{-4}$ (1.09×)

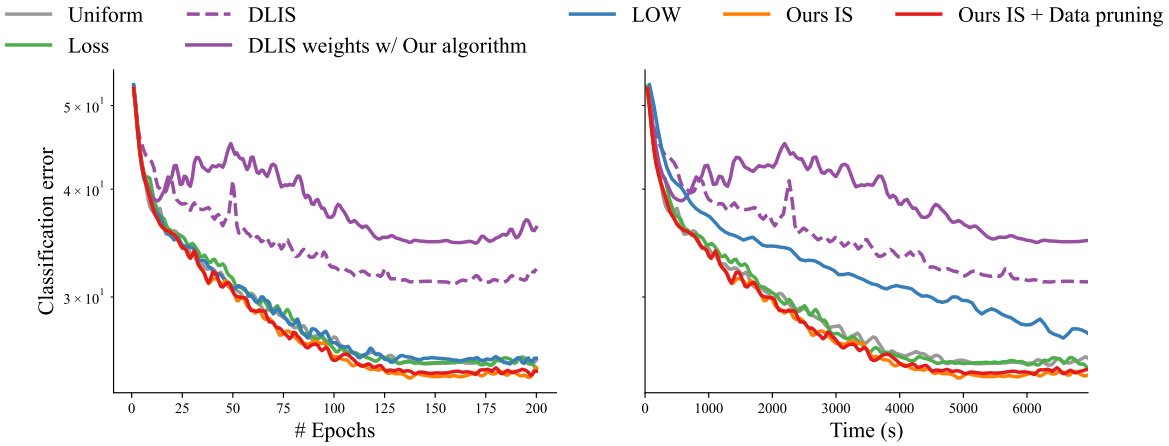


Figure 5: Comparisons on CIFAR-10 using Vision Transformer (ViT) (Dosovitskiy et al., 2021). The results show consistent improvement of Ours IS and Ours IS + Data pruning over LOW (Santiago et al., 2021) and DLIS (Katharopoulos and Fleuret, 2018) for both equal epoch and equal time.

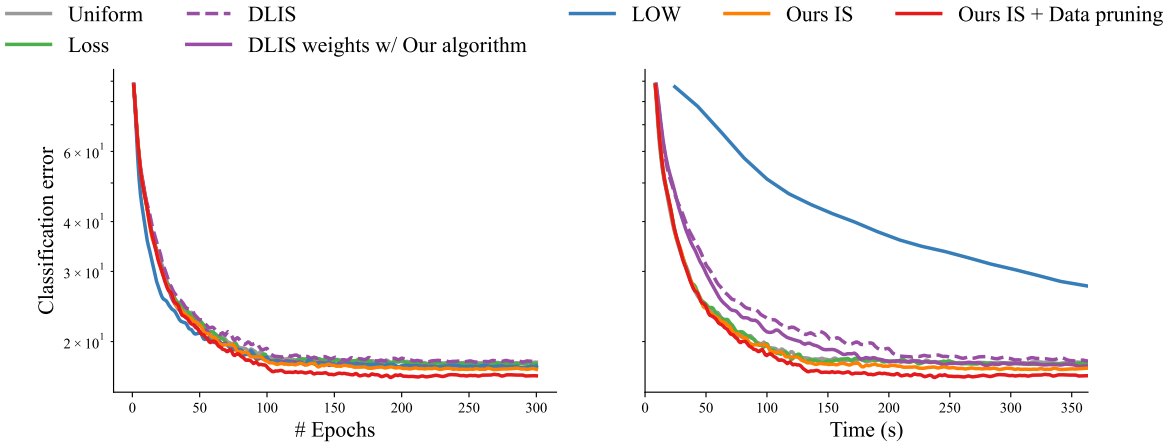


Figure 6: When comparing on the Point cloud (ModelNet40 (Wu et al., 2015)) classification dataset, DLIS performs poorly at equal time due to the resampling overhead. Unlike DLIS (Katharopoulos and Fleuret, 2018), we use standard uniform sampling which is faster. We also compare against another adaptive scheme by Santiago et al. (2021) (LOW). Our importance sampling (Ours IS) with data pruning (Ours IS + Data pruning) show improvements on the ModelNet40 dataset against other methods. achieving lower classification errors with minimal overhead compared to others.

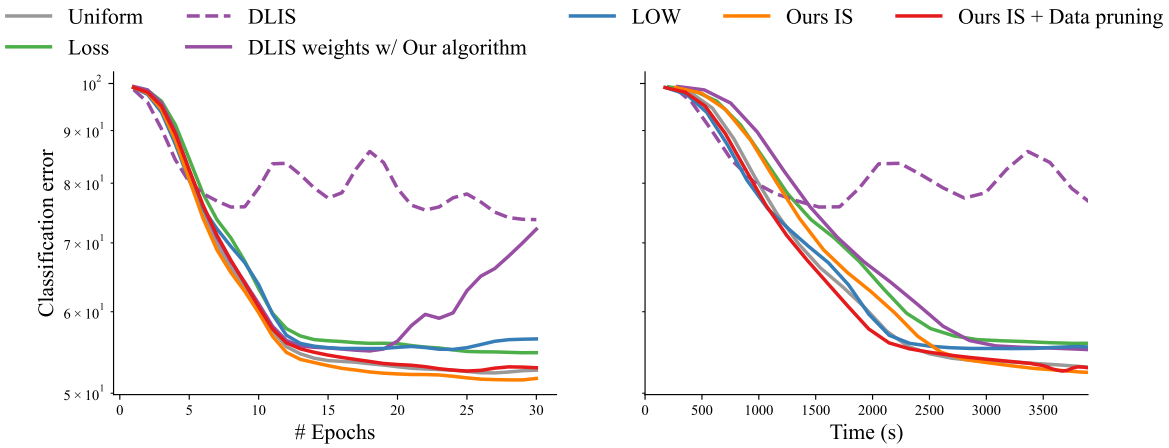


Figure 7: Comparisons on Tiny-ImageNet (Le and Yang, 2015). The results show improvement of our importance sampling (Ours IS) over other methods, while in this case Ours IS with data pruning works similarly to Uniform sampling.

Table 3: We compare the impact of importance sampling (IS) with and without data pruning on classification and regression tasks. Our approach consistently outperforms on majority of datasets. Bold numbers represents the best scores, underlined ones represent the second best. Worse to best for each metric is shown from red to green.

Dataset	Method	Equal step			Equal time	
		Loss (↓)	Accuracy (↑)	Time(s)(↓)	Loss	Accuracy
MNIST	Uniform	0.00092	97.5	477	0.00097	97.4
	Loss IS	0.00083	97.8	474	0.00086	97.7
	DLIS	0.00106	98.0	754	0.00124	97.7
	DLIS weights **w/ Our algorithm**	0.00083	97.8	665	0.00089	97.6
	LOW	0.00072	98.1	624	0.00077	98.0
	Our IS	0.00083	97.8	395	0.00085	97.7
	Our IS + Data pruning	**0.00056**	**98.3**	**386**	**0.00059**	**98.2**
CIFAR-10	Uniform	0.0037	92.5	5810	0.0037	92.4
	Loss IS	0.0060	84.6	5797	0.0057	82.6
	DLIS	0.0055	84.6	5963	0.0036	89.1
	DLIS weights **w/ Our algorithm**	0.0105	63.1	5934	0.0127	53.7
	LOW	0.0036	92.5	10768	0.0039	91.0
	Our IS	0.0038	92.6	5836	0.0036	92.4
	Our IS + Data pruning	**0.0034**	**92.8**	**4395**	**0.0034**	**92.8**
CIFAR-10 (ViT)	Uniform	0.00794	74.6	7105	0.00789	74.8
	Loss IS	0.00790	74.7	**7039**	0.00779	75.1
	DLIS	0.00932	67.6	9111	0.00917	68.2
	DLIS weights **w/ Our algorithm**	0.01050	63.6	8916	0.01000	65.1
	LOW	**0.00762**	74.6	13046	0.00788	73.7
	Our IS	0.00785	**75.5**	7113	**0.00769**	**75.7**
	Our IS + Data pruning	0.00786	75.2	7213	0.00785	75.3
CIFAR-100	Uniform	0.012	72.6	4748	0.012	73.8
	Loss IS	0.023	40.2	4404	0.026	32.8
	DLIS	0.015	62.0	4501	0.015	60.8
	DLIS weights **w/ Our algorithm**	0.021	43.6	4603	0.029	26.3
	LOW	0.011	**74.6**	4730	0.011	74.2
	Our IS	0.011	74.3	4686	0.012	74.3
	Our IS + Data pruning	**0.011**	74.3	**3150**	**0.011**	**74.3**
Flower-102	Uniform	**0.00658**	**79.8**	6327	**0.00658**	**79.8**
	Loss IS	0.01777	57.4	5909	0.01777	57.4
	DLIS	0.02128	46.9	7399	0.01951	43.8
	DLIS weights **w/ Our algorithm**	0.72899	30.9	7504	0.33971	27.8
	LOW	0.00773	76.1	8241	0.00755	76.7
	Our IS	0.00689	79.5	6263	0.00689	79.5
	Ours IS + Data pruning	0.01353	73.6	**3356**	0.01353	73.6
Point cloud	Uniform	0.00505	82.3	356	0.00505	82.2
	Loss IS	0.00495	82.6	358	0.00496	82.5
	DLIS	0.00595	81.9	580	0.00603	81.8
	DLIS weights **w/ Our algorithm**	0.00481	82.6	561	0.00485	82.5
	LOW	0.00572	82.6	4714	0.01173	74.9
	Our IS	0.00480	82.9	374	0.00480	82.9
	Our IS + Data pruning	**0.00478**	**83.2**	**354**	**0.00478**	**83.1**
Tiny-ImageNet	Uniform	0.02176	47.4	7602	0.02176	47.4
	Loss IS	0.02237	45.2	8407	0.02238	45.2
	DLIS	0.03433	26.3	7897	0.03433	26.3
	DLIS weights **w/ Our algorithm**	0.03454	26.1	9300	0.02778	35.0
	LOW	0.02344	43.5	7702	0.02344	43.5
	Our IS	**0.02127**	**48.1**	8461	**0.02123**	**48.5**
	Our IS + Data pruning	0.02193	47.1	**4349**	0.02193	47.1
Image regression	Uniform	9.44	-	**2308**	9.44	-
	Loss IS	11.01	-	2360	11.12	-
	DLIS	14.27	-	2949	15.78	-
	DLIS weights **w/ Our algorithm**	8.44	-	2863	9.37	-
	Our IS	8.13	-	2912	9.16	-
	Our IS + Data pruning	**8.01**	-	2328	**8.05**	-